Study of Vibration Analysis of a Rotating Homogeneous Thermoelastic Circular Disk by using FEM

J. N. Sharma
Department of Mathematics
National Institute of Technology
Hamirpur
H.P 17705 (INDIA)

Dinkar Sharma
Department of Mathematics
Dr. B. R. Ambedkar National
Institute of Technology,
Jalandhar-144011 (INDIA)

Sheo Kumar
Department of Mathematics
Dr. B. R. Ambedkar National
Institute of Technology,
Jalandhar-144011 (INDIA)

ABSTRACT
This paper considers the application of finite element method for the analysis of thermoelastic characteristics of a thin circular disk which is further subjected to a thermal load and an inertia force arising due to rotation of the disk. On the basis of the two dimensional thermoelastic theories, the axisymmetric problem is formulated in terms of second order ordinary differential equation which is solved by FEM. Further, it is assumed that the disk is vibrating. The effect of Kibel number on different components of stress, strain and displacement has also been discussed. The numerical results reveal that these quantities are significantly influenced by temperature distribution and angular speed of the disk.

Keywords
FEM; Circular disk; Axisymmetric; Heat Conduction, Kibel number;

1. INTRODUCTION
Rotating disks are important components in various mechanical applications such as circular saws, disk brakes, hard disks, optical discs and gas turbines. These are often subject to loading or excitation in the transverse (out-of-plane) direction. Analysis of rotating disks has been studied by a number of researchers. Afsar and Go [1] analysed thermoelastic characteristics of a thin circular FGM rotating disk having a concentric hole and subjected to a thermal load. Yongdong *et al.* [2] and Zhong and Yu [3] established a mechanical model for the functionally gradient material (FGM) beam with rectangular cross section and also discussed the effects of the non-homogeneity parameter on the distribution of the normal stress and on the position of the natural axis for several different loading cases. Lamb and Southwell [4], have reported a study on the free vibration of flexible disk and obtained the solution for complete disk of uniform thickness, accounting for the effects of centrifugal and bending stresses. Eversman and Dodson [5] studied the free vibration of a centrally clamped spinning disk. Shahbab [6] analyzed the transverse vibrations of a spinning flexible variable thickness disc. He employed both Ritz method and finite element technique and also carried out experimental investigation. An analytical solution in order to study deformation of a rotating disk composed of a linear, elastic, isotropic and homogeneous material by application of mechanical and thermal load have been studied thoroughly by Timoshenko and Goodier [7].

Benson [8] discussed the steady deflection of a transversely loaded, extremely flexible spinning disk using a hybrid of membrane and late theories when bending stiffness of the disk is small. Chen and Bogy [9] obtained the derivatives of the eigen values of a flexible spinning disk with a stationary load with respect to certain parameters in the system. Further, in another study Mote [10] has also been developed finite element method (FEM) procedures for plates with significant membrane stresses. Nigh and Olson [11] presented a FEM formulation for analysis of disks either in a body-fixed or a space-fixed co-ordinate system.

Finite Element Method (FEM) is one of the most successful and dominant numerical method in the last century. It is extensively used in modeling and simulation of engineering and science due to its versatility for complex geometries of solids and structures and its flexibility for many non-linear problems. The FEM is regarded as relatively accurate and versatile numerical tool for solving differential equations that model physical phenomenon [12-13]. The FEM is closely related to the classical variational concept of the Rayleigh Ritz method [14, 15].The finite element method is well addressed and needs less computation in addition to high accuracy in literature. In the present paper finite element technique is used to evaluate the different components of stress, strain and displacement for two different cases of temperature distributions.

2. MATHEMATICAL MODEL
A circular disk with a concentric circular hole as shown in Figure 1 has been studied. The disk is assumed to be rotating with angular frequency Ω . The origin of the polar co-ordinate system $r-\theta$ is assumed to be located at the center of the disk and hole.

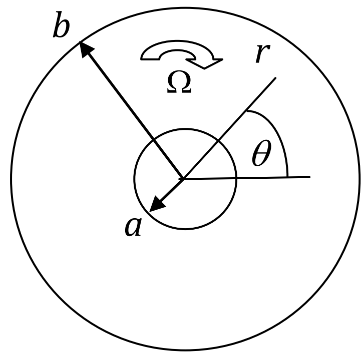

Figure. 1: Schematic diagram of a rotating disk with concentric circular hole

3. BOUNDARY CONDITIONS

The disk considered in the present study is subjected to a temperature gradient field. The inner surface of the disk is assumed to be fixed to a shaft so that isothermal conditions can be prevailed on it. The outer surface of the disk is free from any mechanical load and maintained at uniform temperature gradient. Thus, the boundary conditions of the problem are given by:

(i) $r = a,\ u_r = 0, T = 0$

(ii) $r = b,\ \sigma_r = 0, \dfrac{dT}{dr} = T_0$ (1)

where u_r and σ_r denote displacement and stress along the radial direction.

4. FORMULATION OF THE PROBLEM

When a material is subjected to a temperature gradient field, it experiences a stress arising from an incompatible eigen-strain. Eigenstrains (Dhaliwal and Singh [16]) are non-elastic strains or free expansion strains that develop in a body due to various reasons, such as phase transformation, precipitation, temperature change, etc. in the present study, the eigenstrain is associated with the thermal expansion of the disk. Since the material of the disk is isotropic, the thermal eigenstrain at a point is the same in all directions which can be given by

$$\varepsilon^* = \alpha(r)T(r) \tag{2}$$

Where $T(r)$ is the change in temperature at any distance r. The total strain is the sum of the elastic strain and the eigen strain. Thus, the components of the total strain are given by

$$\varepsilon_r = e_r + \varepsilon^*,\ \varepsilon_\theta = e_\theta + \varepsilon^* \tag{3}$$

Where ε_r and ε_θ are the radial and circumferential component of the total strain and e_r and e_θ are the radial and circumferential components of the elastic strain. The elastic strains are related to stresses by Hooke's law. Thus

$$\varepsilon_r = \frac{1}{E}\left(\sigma_r - \nu\sigma_\theta\right) + \varepsilon^*;$$
$$\varepsilon_\theta = \frac{1}{E}\left(\sigma_\theta - \nu\sigma_r\right) + \varepsilon^* \tag{4}$$

Where σ_r and σ_θ are the radial and circumferential stress components, respectively. The two dimensional equilibrium equation in polar coordinates the inertia force due to rotation of the disk is given by

$$\frac{\partial\sigma_r}{\partial r} + \frac{1}{r}\frac{\partial\tau_{r\theta}}{\partial\theta} + \frac{\sigma_r - \sigma_\theta}{r} + \rho(\omega^2 + \Omega^2)r = 0$$
$$\frac{\partial\tau_{r\theta}}{\partial r} + \frac{1}{r}\frac{\partial\sigma_\theta}{\partial\theta} + \frac{2\tau_{r\theta}}{r} = 0 \tag{5}$$

where Ω is angular rotation of the disk and ω is being the angular frequency of the vibration modes in the disk. Because of symmetry, $\tau_{r\theta}$ vanishes and σ_r, σ_θ are independent of θ. Thus, the second Eq. (5) is identically satisfied and the first equilibrium equation is reduced to

$$\frac{d}{dr}(r\sigma_r) - \sigma_\theta + \rho(\omega^2 + \Omega^2)r = 0 \tag{6}$$

Now, substitute $F = r\sigma_r$ into Eqs. (6) and (4) gives

$$\sigma_\theta = \frac{dF}{dr} + \rho(\omega^2 + \Omega^2)r^2$$
$$\varepsilon_r = \frac{1}{E}\left(\frac{F}{r} - \nu\frac{dF}{dr}\right) - \frac{\nu\rho}{E}\omega^2 r^2 + \varepsilon^*;$$
$$\varepsilon_\theta = \frac{1}{E}\left(\frac{dF}{dr} - \frac{\nu F}{r}\right) + \frac{\rho}{E}\omega^2 r^2 + \varepsilon^* \tag{7}$$

Strain-displacement relations for the axisymmetric problem are

$$\varepsilon_r = \frac{du_r}{dr},\ \varepsilon_\theta = \frac{u_r}{r} \tag{8}$$

From Eq. (8), it is seen that two strain components are related by $\varepsilon_r = \dfrac{d}{dr}(r\varepsilon_\theta)$. By making use of Eq. (7) into this relation, we get

$$\frac{d^2F}{dr^2} + \frac{1}{r}\frac{dF}{dr} - \frac{1}{r^2}F + \rho\Omega^2 r(1+\Gamma^2)(3+\nu) + E\alpha\frac{dT}{dr} = 0 \tag{9}$$

where $\Gamma = \dfrac{\omega}{\Omega}$ is called Kibel number.

The heat conduction equation for a dynamic coupled thermoelastic solid is given by [Dhaliwal and Singh [18]]

$$K\left(\frac{\partial^2}{\partial r^2} + \frac{1}{r}\frac{\partial}{\partial r}\right)T - \rho C_e\frac{\partial T}{\partial t} = \frac{E\alpha T_0(\dot{e}_r + \dot{e}_\theta)}{1-\nu} \tag{10}$$

where K is the thermal conductivity, C_e -Specific heat at constant strain and T_0 being uniform reference temperature. The equations (9) and (10) constitute the mathematical model consisting of second order differential equations which provides us the function F and the components of stress.

5. TEMPERATURE FIELD

We shall consider following three cases of thermal variations in the disk:

Case I: Disk having uniform temperature distribution.
In this case, we have

$$T(r) = T_0, \frac{dT}{dr} = 0 \tag{11}$$

Case II: Disk at steady state temperature distribution.

In this case $\dfrac{\partial}{\partial t} \cong 0$, so that the heat conduction equation (10) takes the form

$$\left(\frac{d^2}{dr^2}+\frac{1}{r}\frac{d}{dr}\right)T=0$$

Upon solving this equation with the help of thermal conditions (4), we obtain

$$T(r)=bT_0\log(r/a)\,,\frac{dT}{dr}=\frac{bT_0}{r} \qquad (12)$$

These temperature distributions given by Eqs.(11) and (12) holds in the domain $a \le r \le b$.

6. FINITE ELEMENT FORMULATION

Substituting the values of T and $\frac{dT}{dr}$ from equations (11) and (12) in Eq. (9) and following a standard finite element discretization approach, the domain of the disk is divided radially into N number of elements of equal size and above Eq. (9) can be transformed to the following system of simultaneous algebraic equations:

$$\sum_{j=1}^{2}K_{ij}^{e}F_{j}^{e}=L_{i}^{e};\ i=1,2:e=1,2,...,N \qquad (16)$$

where

$$K_{ij}^{e}=\int_{r_e}^{r_{e+1}}\frac{d\phi_i^e}{dr}\frac{d\phi_j^e}{dr}dr-\int_{r_e}^{r_{e+1}}\frac{1}{r}\phi_i^e\frac{d\phi_j^e}{dr}dr+\int_{r_e}^{r_{e+1}}\frac{1}{r^2}\phi_i^e\phi_j^e dr$$

$$L_i^e=\int_{r_e}^{r_{e+1}}\phi_i^e f(r)dr+\phi_i^e(r_{e+1})\frac{d\phi_j^e}{dr}(r_{e+1})-\phi_i^e(r_e)\frac{d\phi_j^e}{dr}(r_e)$$

$$f(r)=\rho\Omega^2 r(\nu+3)(1+\Gamma^2)\text{; (Case-I)}$$

$$f(r)=E\alpha\frac{bT_0}{r}+\rho\Omega^2 r(\nu+3)(1+\Gamma^2)\text{; (Case-II)}$$

$$\phi_1^e=\frac{r_{e+1}-r}{r_{e+1}-r_e};\ \phi_2^e=\frac{r-r_e}{r_{e+1}-r_e} \qquad (17)$$

The symbol e used in the above equation indicates the element number which is used to discretize the domain of the disk.

$$\sigma_r=\frac{1}{r}\sum_{j=1}^{2}F_j^e\phi_j^e \quad ,$$

$$\sigma_\theta=\sum_{j=1}^{2}F_j^e\frac{d\phi_j^e}{dr}+\rho\Omega^2 r^2(1+\Gamma^2)$$

$$\varepsilon_r=\frac{1}{E}\sum_{j=1}^{2}\left[\frac{F_j^e\phi_j^e}{r}-\nu F_j^e\frac{d\phi_j^e}{dr}\right]-\frac{\nu\rho\Omega^2 r^2(1+\mathrm{T}^2)}{E}+\varepsilon^*$$

$$\varepsilon_\theta=\frac{1}{E}\sum_{j=1}^{2}\left[F_j^e\frac{d\phi_j^e}{dr}-\frac{\nu}{r}F_j^e\phi_j^e\right]+\frac{\nu\rho\Omega^2 r^2(1+\Gamma^2)}{E}+\varepsilon^*$$

$$u_r=\frac{r}{E}\sum_{j=1}^{2}\left[F_j^e\frac{d\phi_j^e}{dr}-\frac{\nu}{r}F_j^e\phi_j^e\right]+\frac{\nu\rho\Omega^2 r^3(1+\Gamma^2)}{E}+r\varepsilon^*$$

7. RESULTS AND DISCUSSIONS

The variation of radial stress, radial strain, circumferential stress, circumferential strain, and displacement for different values of r with Kibel for first cases has been shown in Figures 2-6. Figure 2 illustrates the variation of radial stress with change in Kibel number for case I at different values of r. Radial stress is increasing in magnitude with the increase in Kibel number for all the three values of r. The value of radial stress is maximum in magnitude for minimum r value and minimum for maximum r value and the intermediate value of radial stress lie for the r = 0.5 mm.

The variation of circumferential stress with Kibel number at different values of r has been shown in Figure 3. An increase in circumferential stress is observed with the increase in values of r. It is observed from the figure that circumferential stress is maximum for the maximum value of r ie r = 0.7mm. The circumferential stress is varied lineraly with increase in Kibel number for all values of r. The circumferential stress starts decreasing as the kibel number crosses to 1 for r = 0.3mm and r = 0.5 mm but for r = 0.7 mm, it starts increasing. The effect of kibel number on radial strain for different values of r is ilustraited in Figure 4. It has been observed from the figure that Radial strain increases with increase in kebel number for r = 0.3 mm and r = 0.5 mm but the behaviour is opposite for r = 0.7 mm. The behaviour of circumferential strain is opposite of the radial strain as illustrated in Figure 5. The circumferential strain decreases with increase in Kibel number for r = 0.3mm and r = 0.5 mm and increases for r = 0.7 mm. The variation of displacement with Kibel number is reported in Figure 6. The displacement is varied linearly with Kibel number for all the cases. The value of displacement is maximum for r = 0.7 mm and minimum for r = 0.3 mm.

The variation of radial stress, radial strain, circumferential stress, circumferential strain, and displacement for different values of r with Kibel for IInd case has been shown in Figures 7-11. From Figure 7, is has been observed that radial stress is maximum in magnitude for r = 0.3 mm as for the first case but the values of radial stress are not closer for all values of Kibel number. The radial stress is increased at a regular interval with different r values. It is observed from the Figure 8 that the values of circumferential stress is negative for r = 0.3 mm and r = 0.5 and positive for r = 0.7 mm. For all three values of r, circumferential stress is decreasing linearly with increase in Kibel number. In Figure 9, variation of radial strain with Kibel number for three values of r has been reported. The radial strain is positive for all values of r in case I but for the case II, it is positive for r = 0.3 mm and r = 0.5 mm. Variation of circumferentail strain with Kibel number at different values of r has been shown in Figure 10. The circumferentail strain follow the order as it has minimum value for r = 0.5 mm and the maximum for r = 0.7 mm. In Figure 11, variation of displacement has been shown with increase in Kibel number. The values of displacement are quite closer for r = 0.3 mm and r = 0.5 mm and varied linearly with Kibel number. For r = 0.7 mm, displacement attained a maximum value.

8. CONCLUSIONS

An analytical solution for thermoelasticity equilibrium equations of a thin axisymmetric rotating disk made of an isotropic material is presented. The variation of different components of stress, strain and displacement in radial direction is measured by applying thermal load with the help of finite element method. It is found that the thermoelastic field in disk is significantly influenced by the temperature distribution profile. Thus, the thermoelastic field in a disk can be controlled and optimized by controlling these parameters. Finally the model is helpful in designing circular cutter or grinding disk.

9. ACKNOWLEDGMENTS

The author Dinkar Sharma thankfully acknowledges the financial assistance provided by MHRD, GOI, New Delhi.

10. REFERENCES

[1] A.M. Afsar, J. Go, Finite element analysis of thermoelastic field in a rotating FGM circular disk, Appl. Math. Mod. 34, 3309-3320 (2010).

[2] L. Yongdong, Z. Hongcai, Z. Nan, D. Yao, Stress analysis of functionally gradient beam using effective principal axes, Int. J. Mech. Mater. 2, 157-164 (2005).

[3] Z. Zhong, T. Yu, Analytical solution of a cantilever functionally graded beam, Compos. Sci. Technol. 67, 481-488 (2007).

[4] H. Lamb, R. V. Southwell, The vibrations of a spinning disk, Proceedings of the Royal Society (London) 99, 272-280 (1922).

[5] W. Eversman, R. O. Dodson, Free vibration of a clamped spinning circular disk, American Institute of Aeronautics and Astronautics Journal, 7, 2010-2012 (1969).

[6] A. A. S. Shahbab, Finite element analysis for the vibration of variable thickness disks, J. Sou.Vib. 162, 67-68 (1993).

[7]] S.P. Timoshenko, J.N. Goodier, Theory of elasticity, Tata McGraw-Hill, 3rd Edition, New York (1970).

[8] R.C. Benson, Observations on the steady-state solution of an extremely flexible spinning disk with transverse load, J. Appl. Mech. 50, 525-530 (1983).

[9] J.S. Chen, D.B. Bogy, Effects of load parameters on the natural frequencies and stability of a flexible spinning disk with a stationary load system. J. Appl. Mech. 59, S230-S235 (1992).

[10] C.D. Mote Jr, Stability control analysis of rotating plates by finite element: emphasis on slots and holes, J. Dyn. Sys. Meas. Control 94, 64-70 (1972).

[11] G.L. Nigh, M.D. Olson, Finite element analysis of rotating disks, J. Sou. Vib. 77, 61-78 (1981).

[12] J.N. Reddy, An Introduction to the Finite Element Method, Tata McGraw-Hill, 3rd Edition, 2005.

[13] D.V. Hutton, Fundamental of Finite Element Analysis, Tata McGraw-Hill, 1st Edition, 2004.

[14] T.J. Chung, Finite element analysis in fluid dynamics, McGraw Hill, New York, 1978.

[15] J. Turner, R.W. Clough, H. C. Martin, L.P. Topp, Stiffness and deflection analysis of complex structures, J. Aero. Sci. 23, 805-823 (1956)

[16] R.S. Dhaliwal, A. Singh, Dynamic Coupled Thermoelasticity, Hindustan Publishing Corporation New Delhi - (India).

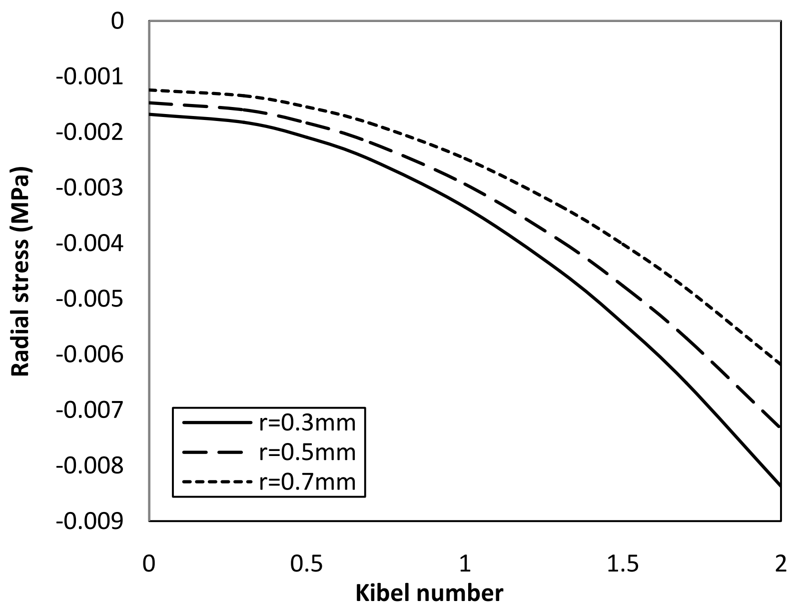

Figure 2. Radial Stresses versus Kibel number for Case I at different values of r .

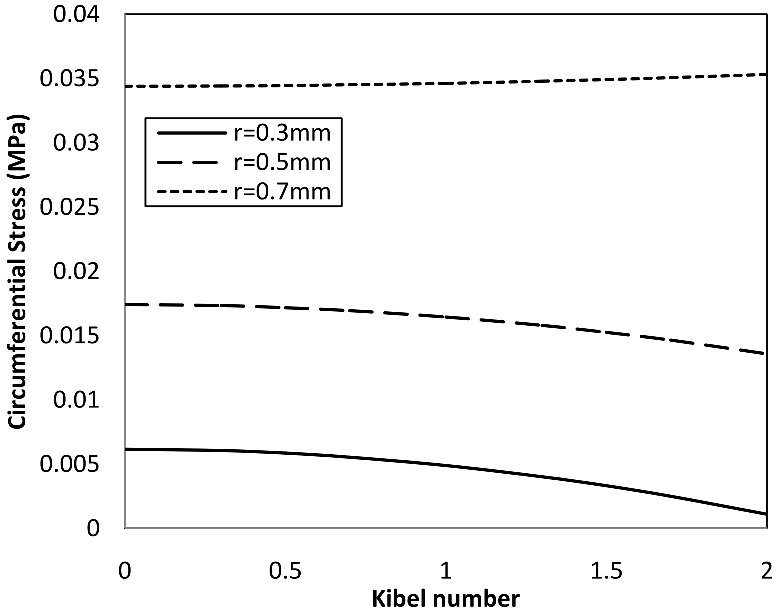

Figure 3. Circumferential Stress versus Kibel number for Case I at different values of r.

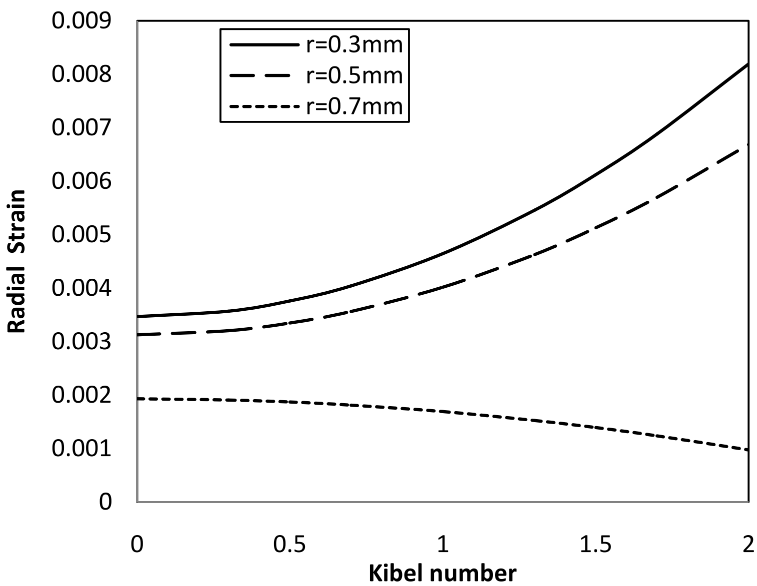

Figure 4. Radial Strain versus Kibel number for Case I at different values of r.

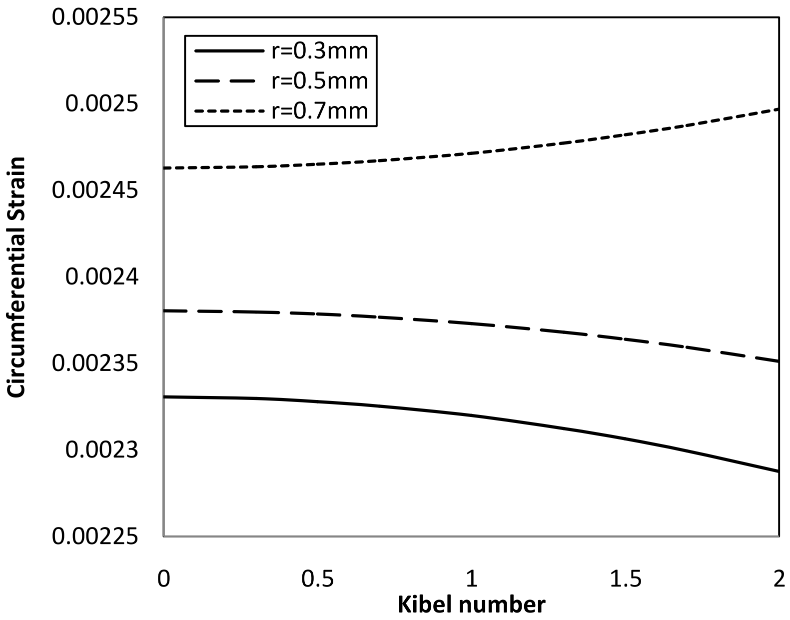

Figure 5. Circumferential Strain versus Kibel number for Case I at different values of r .

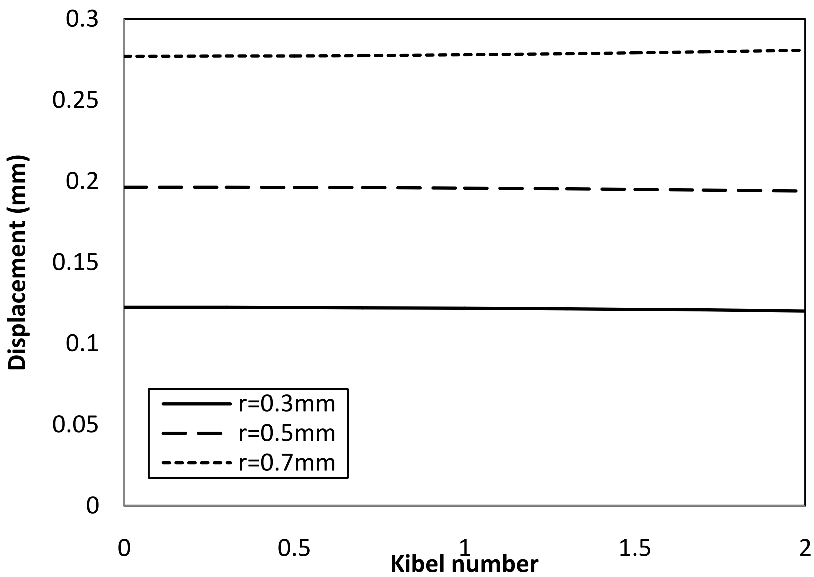

Figure 6. Displacement versus Kibel number for case I at different values of r .

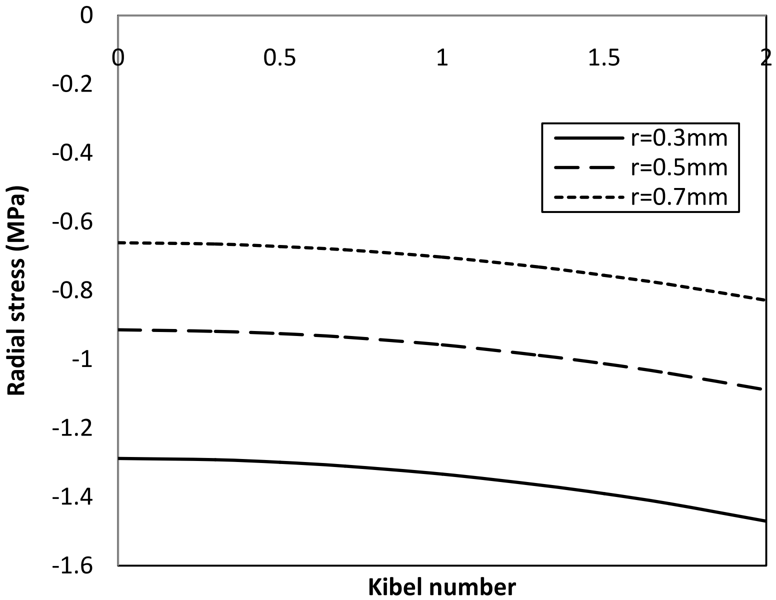

Figure 7. Radial Stresses versus Kibel number for Case II at different values of r **.**

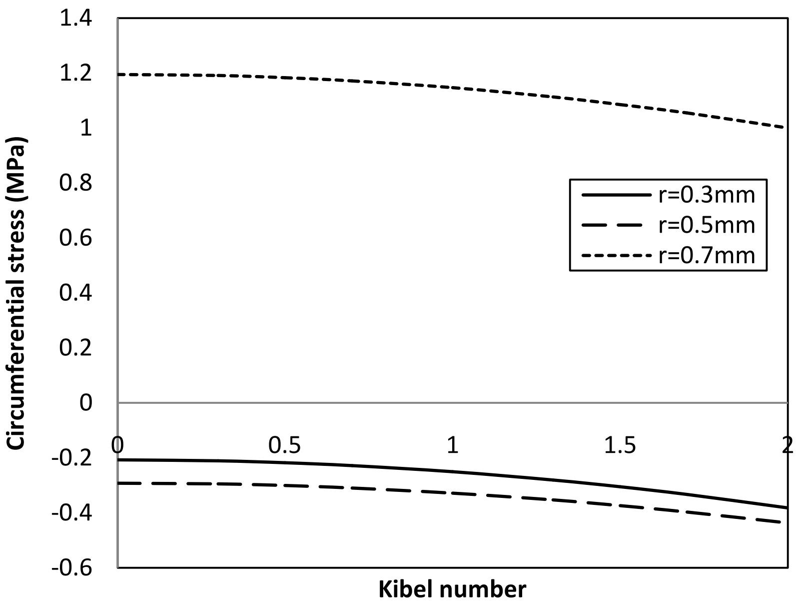

Figure 8. Circumferential Stress versus Kibel number for Case II at different values of r **.**

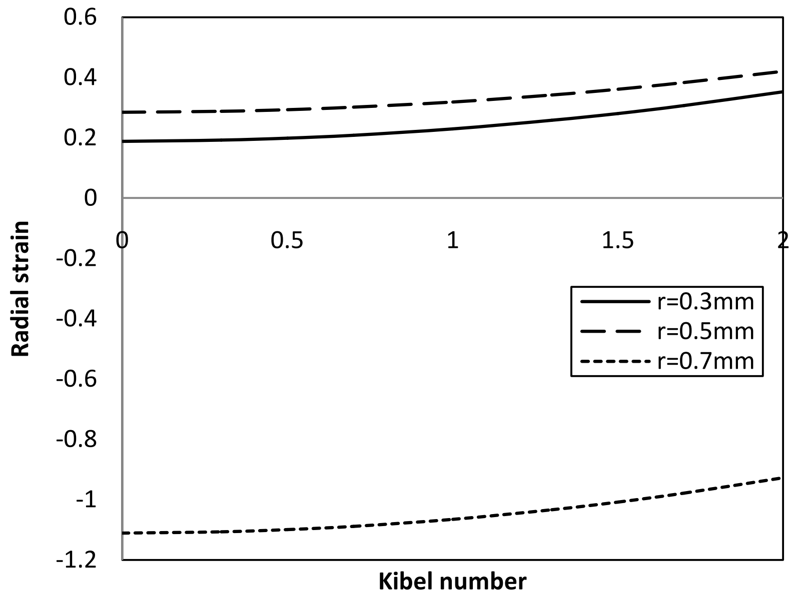

Figure 9. Radial Strain versus Kibel number for Case II at different values of r.

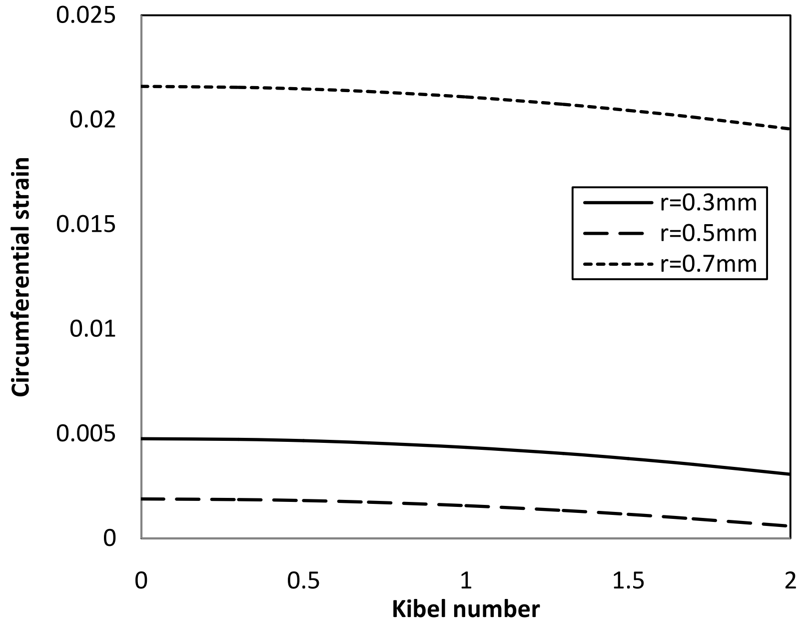

Figure 10. Circumferential Strain versus Kibel number for Case II at different values of r.

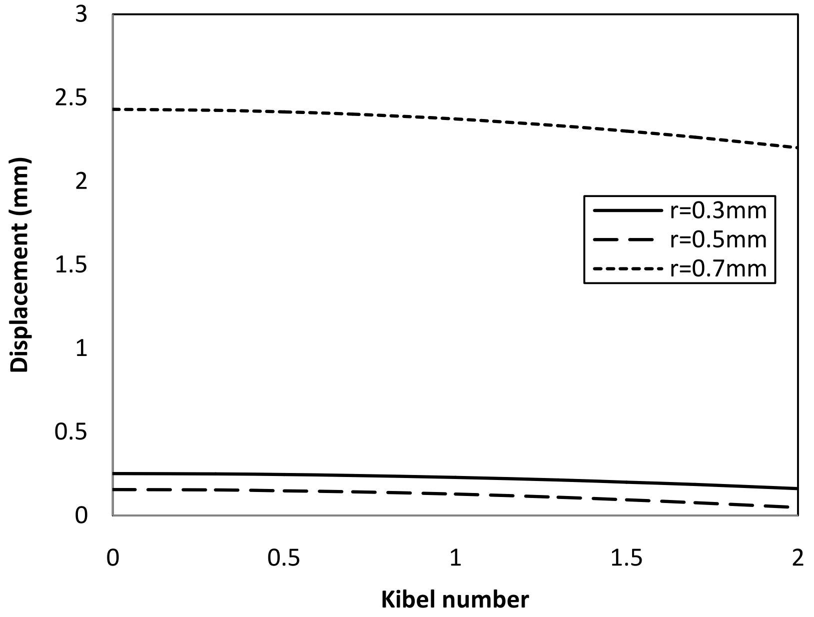

Figure 11. Displacement versus Kibel number for Case II at different values of r **.**